Physics Letters A 380 (2016) 4018–4021

Contents lists available at ScienceDirect

Physics Letters A

www.elsevier.com/locate/pla

Near field evidence of backward surface plasmon polaritons on negative index material boundaries

Mauro Cuevas [a,d,*], Vivian Grunhut [b,d], Ricardo A. Depine [c,d]

[a] Facultad de Ingeniería y Tecnología Informática, Universidad de Belgrano, Villanueva 1324, C1426BMJ, Buenos Aires, Argentina
[b] Facultad de Ingeniería, Universidad Austral, Argentina
[c] Grupo de Electromagnetismo Aplicado, Departamento de Física, FCEN, Universidad de Buenos Aires and IFIBA, Ciudad Universitaria, Pabellón I, C1428EHA, Buenos Aires, Argentina
[d] Consejo Nacional de Investigaciones Científicas y Técnicas (CONICET), Argentina

ARTICLE INFO

Article history:
Received 28 May 2016
Received in revised form 10 September 2016
Accepted 11 October 2016
Available online 14 October 2016
Communicated by V.A. Markel

Keywords:
Surface plasmon polaritons
Negative index material
Metamaterials
Plasmonics
Backward propagation

ABSTRACT

We present a detailed analysis about the electromagnetic response of a metamaterial surface with a localized defect. The excitation of electromagnetic surface waves leads to a near-field distribution showing a periodic dependence along the metamaterial surface. We find that this periodic pattern provides a direct demonstration of the forward or backward surface wave propagation.

1. Introduction

A property of conventional materials that exhibit a real negative electric permittivity — such as metals — is their capacity to guide surface plasmon polaritons (SPPs) along their boundary [1]. SPPs are waves trapped at the interface whose electromagnetic fields decay exponentially into both media. On a single plane interface, the electromagnetic wave is backward inside the metal, i.e., the direction of the energy flux parallel to the interface is opposite to the direction of the wave propagation, but forward on the vacuum side, that is, the direction of the energy flux is the same as the direction of the wave propagation, where the larger fraction of the energy flows. Thus, the net behavior of the SPP in a single metallic surface is always a forward wave for which the total energy flux is in the same direction as the phase velocity [2].

Continuous advances in the realization of negative index materials (NIMs) [3] (artificial media with electric permittivity and magnetic permeability simultaneously negative in the same frequency range), have stimulated a revived interest in the electromagnetic properties of SPPs, and novel characteristics that do not exist in conventional media, such as backward behavior — with a total energy flux, parallel to the interface, that is opposed to the phase velocity — have been reported in Ref. [4]. When the flat boundary of a NIM medium is perturbed with a periodic corrugation, novel SPP radiation characteristics together with new SPP–photon coupling effects, not present in the metallic case, appear [5]. On the other hand, the scattering of light from a topological defect on a metallic surface is currently being investigated, since it provides a convenient way to generate locally SPPs from the incident light [6–8]. One way of characterizing the SPP generation efficiency is by scanning the field near the defect, since its distribution is strongly characterized by the generated SPPs [7,9]. The purpose of this letter is to show that, when a flat boundary is perturbed with a single defect, the near field distribution is related to the forward or backward character of the SPPs excited. In particular, we report near field evidence of backward SPPs, not present in the metallic case, that appear under certain particular conditions on a NIM interface. Within this framework, by using a rigorous method based on Green's second identity [10] for modeling the scattering process, we study the electromagnetic response of an isolated protuberance when illuminated by an electromagnetic, linearly polarized wave. To avoid diffraction effects at the edge of the surface, which must be of finite length in the numeri-

* Corresponding author at: Facultad de Ingeniería y Tecnología Informática, Universidad de Belgrano, Villanueva 1324, C1426BMJ, Buenos Aires, Argentina.
E-mail address: cuevas@df.uba.ar (M. Cuevas).

http://dx.doi.org/10.1016/j.physleta.2016.10.013
0375-9601/

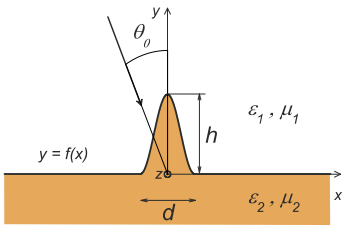

Fig. 1. (Color online.) Schematic illustration of the protuberance and the geometrical parameters.

cal treatment, as in Ref. [10] we assume the incident field to be a beam of finite width.

2. Scattering problem

In Fig. 1, we present schematically a single protuberance showing the geometrical parameters defining the structure and the coordinate axes used. The conventional material is vacuum ($\epsilon_1 = \mu_1 = 1$) and the boundary is a single sinusoidally corrugated as follows: $f(x) = h/2\,[1 + \cos(2\pi/d)]\,\mathrm{rec}(x/d)$ where $\mathrm{rec}(u)$ is the rectangular function centered at the origin with unit width and height. In all the examples presented here, the illumination is accomplished by a Gaussian beam, $\varphi_i(x, y) = e^{-(x\cos\theta_0 + y\sin\theta_0)^2/w^2}\, e^{i\frac{\omega}{c}(x\sin\theta_0 - y\cos\theta_0)}$, where $\varphi_i(x, y)$ is the z-directed component of the total magnetic field (p polarization) or the total electric field (s polarization), w is half of the beam width at the waist, ω is the angular frequency and c is the speed of light in vacuum. The angle of incidence θ_0 of the beam is defined with respect to the y axis. It is known (see Ref. [11], and references therein) that outside the corrugated region ($y > \max f(x)$ or $y < \min f(x)$), the fields can be rigorously represented by superpositions of plane waves,

$$\varphi_1(x, y) = \varphi_i(x, y) + \int_{-\infty}^{+\infty} R(\alpha)\, e^{i(\alpha x + \beta^{(1)}(\alpha) y)}\, d\alpha, \tag{1}$$

for $y > \max f(x)$ and

$$\varphi_2(x, y) = \int_{-\infty}^{+\infty} T(\alpha) e^{i(\alpha x - \beta^{(2)}(\alpha) y)}\, d\alpha, \tag{2}$$

for $y < \min f(x)$, where $R(\alpha)$ and $T(\alpha)$ are complex amplitudes and $\beta^{(j)}(\alpha) = \sqrt{\frac{\omega^2}{c^2}\varepsilon_j\mu_j - \alpha^2}$. Note that the quantities $\beta^{(1)}(\alpha)$ are real or purely imaginary. In the first case, which occurs in the so-called radiative zone $|\alpha| < \omega/c$, the integrand in eq. (1) represents plane waves propagating away from the surface along a direction that forms a scattering angle θ_s [$\sin\theta_s = c\,\alpha/\omega$] with the $+y$ axis. In the second case, which occurs in the so-called non radiative zone $|\alpha| > \omega/c$, these fields represent evanescent waves that attenuate for $y \longrightarrow +\infty$. In the real case of lossy transmission media ($\mathrm{Im}\,\varepsilon_2 > 0$, $\mathrm{Im}\,\mu_2 > 0$), the quantities $\beta^{(2)}(\alpha)$ are always complex with a nonzero imaginary part, $\mathrm{Im}\,\beta^{(2)}(\alpha) > 0$, so that the fields in eq. (2) attenuate for $y \longrightarrow -\infty$. After imposing the boundary conditions, we arrive at the electromagnetic fields above and below the boundary $y = f(x)$. The calculations are obtained using an integral method based on Green's second identity [10] and incorporating the changes made in Ref. [11] in order to include media with negative indices of refraction. According to expression (1), the near field on the vacuum side is a superposition of propagating and evanescent waves, being $R(\alpha)$ the weight of each of them depending on whether $|\alpha| < \omega/c$ or $|\alpha| > \omega/c$, respectively. In order to clarify the role of these waves, we calculate the amplitude $R(\alpha)$.

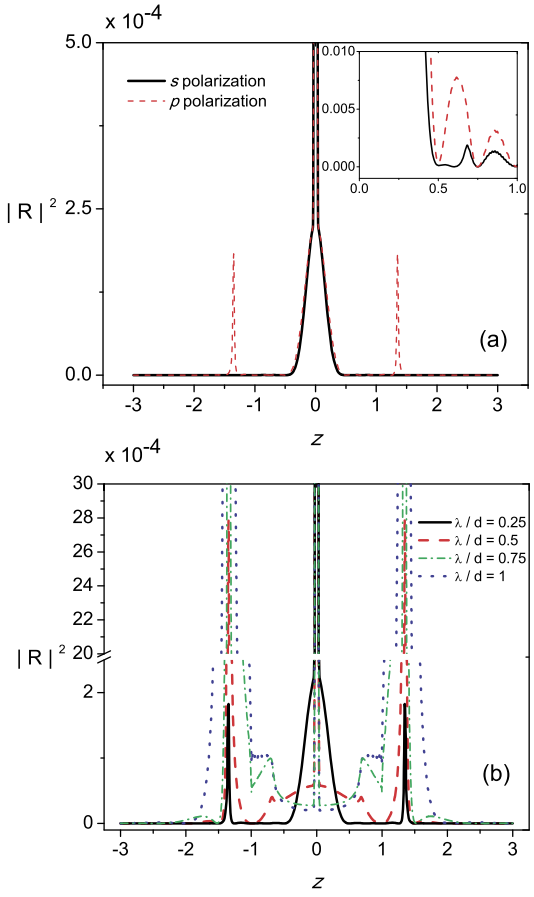

Fig. 2. (Color online.) Curves of $|R(z)|^2$ for a sinusoidal protuberance with $h = 0.012\,\lambda$ illuminated at normal incidence ($\theta_0 = 0$). Width (a) $d = 4\,\lambda$, p and s polarization, (b) $d = 2\lambda,\ 4/3\,\lambda,\ \lambda$, p polarization. The relative constitutive parameters are $\epsilon = -1.3 + i0.01$ and $\mu = -0.35 + i0.01$.

First we consider the constitutive parameters $\epsilon = -1.3 + i0.01$ and $\mu = -0.35 + i0.01$ ($n = -0.674 + i0.012$), for which the flat interface supports a p-polarized forward SPP [4] with a complex dimensionless propagation constant $\kappa = c\,\alpha/\omega = 1.337 + i0.020$. We consider a protuberance with $h = 0.012\,\lambda$ and $d = 4\,\lambda$ ($h/d = 0.003$) where $\lambda = c/(2\pi\,\omega)$ is the wavelength in the vacuum. Fig. 2a shows the square modulus of the complex amplitude $R(z)$ as a function of the dimensionless wave vector $z = c/\omega\,\alpha$ for a normal beam wave incidence ($\theta_0 = 0$) and $w = 20\lambda$. In the radiative zone, $|z| < 1$, the curves are almost identical for both polarizations, with a principal peak whose spectral half width $\Delta z = c/\omega\,(2/w) = 0.1/(2\pi)$, centered at the value of the spectral variable $z = 0$. This peak represents the wave reflected by the flat surface, reaching a maximum value of 50000×10^{-4} [not shown in Fig. 2a]. The presence of the protuberance is manifested by non-zero values of $|R|^2$ in the non-specular direction, reaching a maximum value $\approx 2.5 \times 10^{-4}$ for $z = 0$ and two minima located at $z = \pm 0.5$ (see inset of Fig. 2a). We observe that only the values of $R(z)$ with z between these two minima significantly contribute to the scattered power. Unlike the radiative zone, the curve $|R(z)|^2$ shows a significant difference between the s and p polarizations beyond the radiative zone, as can be seen in Fig. 2a for $|z| > 1$. For p polarization, this curve shows two enhanced maxima at values of $z \approx \pm\,\mathrm{Re}\,\kappa$, indicating that two SPPs, one SPP propagating in $+x$ direction and the other one propagating in $-x$ direction, are excited by the p-polarized incident beam wave. However, there is no maximum for s polarization due to the fact that no SPPs with s polarization are supported by the surface. As we decrease the width of the protuberance d with respect to the

wavelength λ, the presence of the protuberance becomes more evident both in the radiative zone and in the non-radiative zone, as can be seen in Fig. 2b, where we have included the curves of $|R(z)|^2$ with $\lambda/d = 1/2,\ 3/4$, and 1 for p polarization. On the one hand, the power scattered in the non-specular direction is spread toward larger angles. Moreover, we observe that, while the curve for $\lambda/d = 1/4$ has two minima on the radiative zone, at $z = \pm 1/2$, the curves for $\lambda/d = 1/2,\ 3/4$ and 1 have their minima at $z = \pm 1, \pm 1.5$ and ± 2 respectively. The location of these minima coincides with the location of the zeroes corresponding to the Fourier transform of the surface profile, $z = \pm 2\lambda/d$, in agreement with the fact that in the limit of shallow corrugation, the diffracted field amplitude $R(z)$ corresponding with a plane wave incident is proportional to the Fourier transform of the profile $f(x)$ for both polarizations [11]. Although in the above examples the incident field is not a plane wave, the beam impinging on the surface is over $2w = 40\lambda$, largely covering the entire protuberance. Thus the incident wave can be regarded as a plane wave in this case. On the other hand, when λ/d increases from 1/4 to 1, we observe that the peaks located in $|z| \approx \mathrm{Re}\,\kappa$ become more and more pronounced, exhibiting a higher maximum $\approx 3500 \times 10^{-4}$ [not shown in Fig. 2b] for $\lambda/d = 1$. As a consequence, the major contributions to the integrand in eq. (1) are given by the amplitude $R(\pm \mathrm{Re}\,\kappa)$ of the excited SPPs and the amplitude $R(z)$ associated with the reflection by an infinite plane. Given the small value of the spectral width considered in the above examples, each plane wave component of the incident beam undergoes a reflection with identical amplitude as that of the specular component, and therefore $R(z) \approx R_F(\sin\theta_0)$, where R_F is the Fresnel coefficient of the interface. From this fact, it follows that the near field given by eq. (1) on the vacuum side can be approximately represented by the following expression,

$$\varphi_1(x,y) = \begin{cases} \varphi_i(x,y) + \varphi_r(x,y) R_F(\sin\theta_0) \\ \quad + \bar{\mathrm{R}}(-\mathrm{Re}\,\kappa) e^{i(\alpha_- x + \beta^{(1)}(\alpha_-) y)} & y < 0, \\ \varphi_i(x,y) + \varphi_r(x,y) R_F(\sin\theta_0) \\ \quad + \bar{\mathrm{R}}(\mathrm{Re}\,\kappa) e^{i(\alpha_+ x + \beta^{(1)}(\alpha_-) y)} & y > 0, \end{cases} \tag{3}$$

where the sign + and − must be taken for $x > 0$ and for $x < 0$ respectively, $\alpha_+ = \omega\kappa/c$ is the propagation constant of SPP on $x > 0$ side, $\alpha_- = -\omega\kappa/c$ is the propagation constant of SPP on $x < 0$ side, $\bar{\mathrm{R}}(\kappa)$ is the amplitude of the SPP field on $x > 0$ side, $\bar{\mathrm{R}}(-\kappa)$ is the amplitude of the SPP field on $x < 0$ side and

$$\phi_r(x,y) = e^{-(x\,\cos\theta_0 + y\,\sin\theta_0)^2/w^2}\, e^{i\frac{\omega}{c}(x\,\sin\theta_0 + y\,\cos\theta_0)}. \tag{4}$$

This simplified model has been suggested in Ref. [7] where it was used to extract the SPP generation efficiency in the metallic case. Within the framework of this model, the square modulus $|\varphi_1(x,y)|^2$ is a background plus a term $I_\pm$ that contains the cross product between the first two terms with the third one, i.e., the interference of the incident (and reflected) fields with the field of generated SPPs,

$$I_\pm = e^{-2(x\,\cos\theta_0 + y\,\sin\theta_0)^2/w^2}\ \mathrm{Re}\,\{\bar{\mathrm{R}}(\pm\mathrm{Re}\,\kappa) e^{i(\mathrm{Re}\,\alpha_\pm - \alpha_0)x} \times [e^{-i(\beta_0 + \mathrm{Re}\,\beta)y} + R_0^* e^{i(\beta_0 - \mathrm{Re}\,\beta)y}]\} e^{-\mathrm{Im}\,\beta\, y} e^{-\mathrm{Im}\,\alpha_\pm x}, \tag{5}$$

where I_+ and I_- refers to $x > 0$ and $x < 0$, respectively, $\alpha_0 = \frac{\omega}{c}\sin\theta_0$ is the x component of the wave vector of the incident and the reflected field. Eq. (5) shows a periodic spatial dependence along the x-direction, gradually attenuating with the increase of $|x|$, with a decay length $\sim 1/|\mathrm{Im}\,\alpha_\pm|$ owing to losses arising from absorption in the metamaterial medium. The periods at each side of the protuberance are: $d_+ = 2\pi/|\alpha_0 - \mathrm{Re}\,\alpha_+|$ for $x > 0$, and $d_- = 2\pi/|\alpha_0 - \mathrm{Re}\,\alpha_-|$ for $x < 0$. Thus, when the beam impinges on the surface with an angle $\theta_0 \neq 0$, fringes with different periods ($d_+ \neq d_-$) appear at each side of the protuberance.

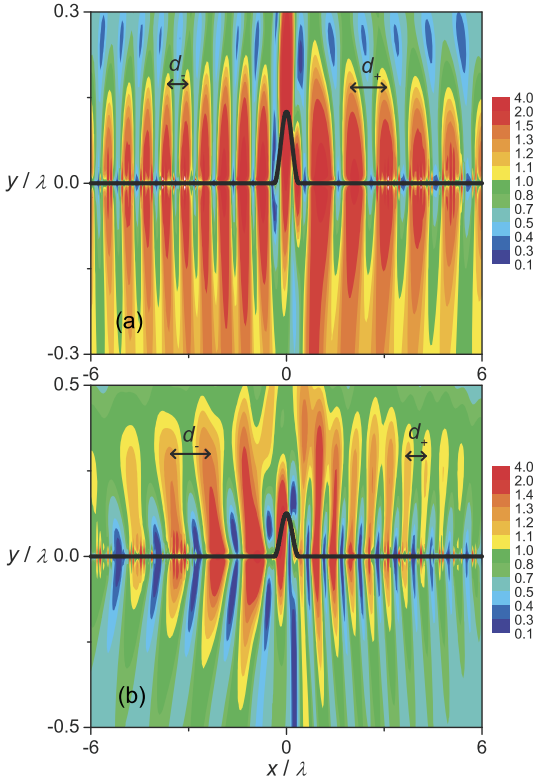

Fig. 3. (Color online.) Map of normalized field $|\varphi(x,y)|$ near the protuberance for a boundary given by $f(x) = h/2\,[1 + cos(2\pi/d)]\,\mathrm{rec}(x/d)$, with $d = 0.75\lambda$ and $h = 0.125\lambda$ separating the vacuum from a NIM medium. a) $\epsilon = -1.3 + i0.01$ and $\mu = -0.35 + i0.01$, the beam width $w = 10\lambda$, $\theta_0 = 20°$ and p polarization. b) $\epsilon = -1.6 + i0.01$ and $\mu = -0.8 + i0.01$, $w = 10\lambda$, $\theta_0 = 30°$ and s polarization.

In order to illustrate this assertion, by using the Green's method, we have calculated the distribution of the magnetic field amplitude (normalized to the amplitude of the incident beam) near the surface for a protuberance with $d = 0.75\lambda$ and $h = 0.125\lambda$ ($h/d = 1/6$) when the illumination is accomplished by a Gaussian beam of width $w = 10\lambda$. Fig. 3a shows the absolute value of the magnetic field near the surface for $\theta_0 = 20°$. Two periodicities are present in the field distribution at each side of the protuberance: i) a rapid variation in the region $x < 0$ from which the incident beam impinges; and ii) a slow variation in the region $x > 0$. This behavior can be understood from the fact that the two excited SPPs, one SPP propagating in $+x$ direction and the other one propagating in $-x$ direction, have their wave vector pointing out of the protuberance. In other words, the propagation constant of excited SPPs propagating on half-space $x > 0$ is $\mathrm{Re}\,\alpha_+ = (\omega/c)\,\mathrm{Re}\,\kappa$ and the propagation constant of excited SPPs propagating on half-space $x < 0$ is $\mathrm{Re}\,\alpha_- = -(\omega/c)\,\mathrm{Re}\,\kappa$ as shown in Fig. 2. Therefore, the period in the half-space $x > 0$ takes a value $d_+ = 2\pi/|\alpha_0 - \mathrm{Re}\,\alpha_+| = \lambda/|\sin\theta_0 - \mathrm{Re}\,\kappa| \approx \lambda/|\sin 20° - 1.34| \approx 1.002\lambda$. On the other hand, in the half-space $x < 0$, the period $d_- = 2\pi/|\alpha_0 - \mathrm{Re}\,\alpha_-| = \lambda/|\sin\theta_0 + \mathrm{Re}\,\kappa| \approx \lambda/|\sin 20° + 1.34| \approx 0.594\lambda$.

It is worth noting that, according to our calculations, the near-field fringes are well-visible for values of d lower than eight times the value of the height ($d < 8h$), and that these fringes are no longer visible for values of $d > 15h$. On the other hand, if we substitute the NIM medium by a metallic medium, the interference pattern will be like as shown in figure 3a [7]. This is true because the forward nature of metallic SPPs.

Another SPP–photon coupling regime which radically differs from what has been known so far for metallic boundaries occurs in the regions of constitutive parameters supporting backward

SPPs. In our next example we consider constitutive parameters $\epsilon = -1.6 + i0.01$ and $\mu = -0.8 + i0.01$ ($n = -1.131 + i0.0106$). Without corrugation, this boundary supports s-polarized backward SPPs with dimensionless propagation constant $\kappa = 1.332 - i0.0379$. By solving the scattering problem for these constitutive parameters, and for protuberance heights in the range considered in the former example, we have verified that, as shown in Fig. 2, in the radiative zone the curves of $|R(z)|^2$ show similar values for both s and p polarizations, and the curve for s polarization reaches a maximum value due to the excitation of SPPs in the vicinity of $|z| = \kappa^R \approx 1.332$. However, as the near field mostly depends on the excited SPPs, the different propagation characteristics between backward SPPs and forward SPPs lead to a spatial distribution of the field that differs from those plotted in Fig. 3a. This is shown in Fig. 3b, where we plot the near electric field distribution for the same geometrical parameters of the protuberance as those in Fig. 3a, but for an angle of incidence $\theta_0 = 30°$ and a beam width $w = 10\lambda$. Unlike the distribution plotted in Fig. 3a, in which the rapidly varying fringes are presented on the left side ($d_- < d_+$), Fig. 3b shows the rapidly varying fringes on the right side ($d_- > d_+$). This difference can be understood by taking into account the fact that the energy carried by the backward SPP is opposite to its propagation direction. For this reason, in backward SPPs the sign of the real part of the propagation constant is opposite to the corresponding imaginary part. As the energy must attenuate, the exponential SPP decay is in the same direction as the total energy flow, that is, the imaginary part of the propagation constant must be positive in the half-space $x > 0$ ($\mathrm{Im}\,\alpha_+ > 0$) and negative in the half-space $x < 0$ ($\mathrm{Im}\,\alpha_- < 0$). Therefore, for $x > 0$ is $\mathrm{Re}\,\alpha_+ < 0$, and for $x < 0$ is $\mathrm{Re}\,\alpha_- > 0$. From the above discussion it follows that the spatial periodicity of the distribution of the near field on the right side of the protuberance is $d_+ = 2\pi/|\alpha_0 - \mathrm{Re}\,\alpha_+| = \lambda/|\sin\theta_0 + \mathrm{Re}\,\kappa| \approx \lambda/|\sin 30° + 1.33| \approx 0.545\lambda$, and on the left side is $d_- = 2\pi/|\alpha_0 - \mathrm{Re}\,\alpha_-| = \lambda/|\sin\theta_0 - \mathrm{Re}\,\kappa| \approx \lambda/|\sin 30° - 1.33| \approx 1.248\lambda$.

3. Conclusions

In conclusion, we have studied the electromagnetic response of a localized protuberance on a NIM interface. Whereas in the radiative zone, the field only depends on geometrical and constitutive parameters of the NIM interface, the electromagnetic field distribution in the vicinity of the protuberance strongly depends on polarization. We have demonstrated that this distribution is highly dependent on the propagation characteristics of the SPP generated and provides an indirect but vivid demonstration of the backward or forward nature of the SPPs.

The possibility to vary the form of the surface defect considering asymmetric structures as well as finite gratings, allows another degree of freedom to modify the SPP spectral peaks. Although we are planning to report the results of such study in a future paper, as a first step we have restricted ourselves to performing an analysis on a single sinusoidally surface defect.

Acknowledgements

The authors acknowledge the financial support of Consejo Nacional de Investigaciones Científicas y Técnicas, (CONICET, PIP 1800) and Universidad de Buenos Aires (project UBA 20020100100327).

References

[1] H. Raether, Surface Plasmons on Smooth and Rough Surfaces and on Gratings, Springer-Verlag, Berlin, 1988.
[2] A. Hohenau, A. Drezet, M. Weißenbacher, F.R. Aussenegg, J.R. Krenn, Phys. Rev. B 78 (2008) 155405.
[3] D.R. Smith, J.B. Pendry, M.C.K. Wiltshire, Science 305 (2004) 788.
[4] S.A. Darmanyan, M. Nevière, A.A. Zakhidov, Opt. Commun. 225 (2003) 233.
[5] M. Cuevas, R.A. Depine, Phys. Rev. Lett. 103 (2009) 097401.
[6] W.L. Barnes, A. Dereux, T.W. Ebbesen, Nature (London) 424 (2003) 14.
[7] B. Wang, L. Aigouy, E. Bourhis, J. Gierak, J.P. Hugonin, P. Lalanne, Appl. Phys. Lett. 94 (2009) 011114.
[8] H. Ditlbacher, J.R. Krenn, A. Hohenau, A. Leitner, F.R. Aussenegg, Appl. Phys. Lett. 83 (2003) 3665.
[9] H.W. Kihm, K.G. Lee, D.S. Kim, J.H. Kang, Q-Han Park, Appl. Phys. Lett. 92 (2008) 051115.
[10] A.A. Maradudin, T. Michel, A.R. McGurn, E.R. Méndez, Ann. Phys. 203 (1990) 255–307.
[11] V. Grünhut, Ricardo A. Depine, Eur. Phys. J. D 62 (2011) 227.